Optical Materials 35 (2013) 2643–2648

Contents lists available at ScienceDirect

Optical Materials

journal homepage: www.elsevier.com/locate/optmat

Femtosecond laser processing of glassy and polymeric matrices containing metals and semiconductor nanostructures

J.M.P. Almeida [a], V. Tribuzi [a], R.D. Fonseca [a], A.J.G. Otuka [a], P.H.D. Ferreira [a], V.R. Mastelaro [a], P. Brajato [a], A.C. Hernandes [a], A. Dev [a,d], T. Voss [b], D.S. Correa [c], C.R. Mendonca [a,*]

[a] Instituto de Física de São Carlos, Universidade de São Paulo, 13560-970, São Carlos, SP, Brazil
[b] Institute of Solid State Physics, University of Bremen, 28359 Bremen, Germany
[c] Laboratório Nacional de Nanotecnologia para o Agronegócio (LNNA), Embrapa Instrumentação, 13560-970, São Carlos, SP, Brazil
[d] School of Information and Communication Technology, Royal Institute of Technology (KTH), Electrum 229, S-16440 Kista, Sweden

ARTICLE INFO

Article history:
Received 8 January 2013
Received in revised form 25 July 2013
Accepted 1 August 2013
Available online 26 August 2013

Keywords:
Femtosecond laser
Material processing
Two-photon polymerization
Metallic nanoparticles
Hybrid nanomaterials

ABSTRACT

Tailoring properties of materials by femtosecond laser processing has been proposed in the last decade as a powerful approach for technological applications, ranging from optics to biology. Although most of the research output in this field is related to femtosecond laser processing of single either organic or inorganic materials, more recently a similar approach has been proposed to develop advanced hybrid nanomaterials. Here, we report results on the use of femtosecond lasers to process hybrid nanomaterials, composed of polymeric and glassy matrices containing metal or semiconductor nanostructures. We present results on the use of femtosecond pulses to induce Cu and Ag nanoparticles in the bulk of borate and borosilicate glasses, which can be applied for a new generation of waveguides. We also report on 3D polymeric structures, fabricated by two-photon polymerization, containing Au and ZnO nanostructures, with intense two-photon fluorescent properties. The approach based on femtosecond laser processing to fabricate hybrid materials containing metal or semiconductor nanostructures is promising to be exploited for optical sensors and photonics devices.

1. Introduction

The need for developing advanced hybrid materials based on polymers, glasses, and ceramics with enhanced properties has increased dramatically in the last few years. Further development for processing such materials in a fast, effective, and low-cost way, however, is still on demand. Among the technologies up-to-date employed for processing hybrid advanced materials, femtosecond laser processing (FLP) [1–5] stands out due to its high precision, low heat generation, and capability to design 2D and 3D structures, providing the materials with new architectures and properties.

The fabrication tailoring of these hybrid materials by FLP depends mainly on the laser intensity. Thus, the use of ultra-short laser pulses (50–150 fs), with pulse energy ranging from nJ to mJ, as well as, tight focusing lens with high NA are required. As FLP involves nonlinear absorption, it is desirable that the material does not absorb the wavelength of the laser. However, it is possible to micromachining the bulk of materials that have electronic transitions close to the energy of the incident photon, in which multi-photon absorption, confined in the focal volume, is responsible for the microstructuring. Ordinary oscillation of the laser beam does not affect the fabrication due to fast processing.

One interesting application for femtosecond laser processing (FLP) regards the fabrication of three-dimensional polymeric micro/nanostructures using two-photon polymerization (2PP) [6,7]. 2PP takes place when two photons are simultaneously absorbed by the chemical species responsible for triggering the polymerization, which consequently hardens the polymeric resin in a well confined spatial region. Considering that 2PP shows a quadratic dependence on the light intensity, as a consequence of the two-photon absorption nature, such process yields high spatial resolution and low light scattering. Another important feature for 2PP is related to the polymerization threshold, which directly influences the generation of radical species. By controlling the laser intensity at the focal volume, one can create radicals by two-photon absorption (2PA), that are neither suppressed by oxygen (which would reduce or hinder voxel growth), nor polymerize large voxels which are not desired for micro/nanofabrication. Therefore, structures with dimensions below the diffraction limit can be obtained [6–8]. For instance, two-photon polymerization has been employed in micro/nanofabrication for applications in optics, biology and microfluidics [3,6,9–14].

* Corresponding author. Tel.: +55 1633738085.
E-mail address: crmendon@ifsc.usp.br (C.R. Mendonca).

0925-3467/$ - see front matter © 2013 Elsevier B.V. All rights reserved.
http://dx.doi.org/10.1016/j.optmat.2013.08.001

Femtosecond laser has also been used for processing glassy materials in order to fabricate two- and three-dimensional structures, including optical components, such as waveguides and resonators [1,15,16]. For microstructuring glasses, one usually takes advantage of FLP to induce nonlinear optical interactions, such as multi-photon absorption or ionization. Such processes involve plasma generation and its subsequent absorption of the laser energy causes irreversible damages to the material [17]. In glasses, such damages can result in a change of the refractive index, absorption coefficient, nonlinear optical susceptibility, structure and local composition [18]. Changes in the valence states of some ions have also been observed, which is useful for the generation of localized nanoparticles in glass with distinct shapes [19,20]. As an example of these applications, the formation of copper nanoparticles in a borosilicate glass by fs-laser micromachining has been demonstrated [21].

Metallic nanoparticles have attracted great attention because of their unique optical and electronic properties. Their use in nanoplasmonics has been proposed for applications in cancer treatments [22,23], chemical and biological sensing [24,25] and photovoltaic cells [26]. By using such nanoparticles it is possible to tailor the optical properties of micro devices, for example through the local field enhancement effect. Furthermore, the characteristic plasmon absorption band is sensitive to the surrounding medium making microdevices doped with nanoparticles suitable for sensor applications. In the same way, semiconductor nanostructures have also been widely exploited for technological applications, in which ZnO nanowires have a fundamental role. Due to its wide-bandgap (3.37 eV) and large exciton binding energy (60 meV), ZnO has been used for the development of UV photodetectors, optical switches and nonlinear frequency converters. Moreover, ZnO nanowires can be used in hybrid structures along with polymeric matrices for fabrication of efficient UV or white LEDs [27].

On an account of quantum confinement effects, many studies have been directed to the incorporation of Au, Ag or Cu nanoparticles and Zno nanowires in different matrices, resulting in a nanocomposite or hybrid material. Although considerable advances have been achieved for the production of macroscopic samples, the preparation of these hybrid materials in the microscopic scale are still on demand.

In this work we report on the use of femtosecond laser for processing new nanocomposites in the micrometer scale, including (i) polymer-based structures, fabricated by 2PP, containing gold or ZnO nanowires, with luminescence properties that can be tuned according to the excitation wavelength and (ii) borate and borosilicate glassy matrices doped with silver and cooper, where metal nanoparticles are produced by the laser irradiation, with interesting optical properties.

2. Experimental

The microfabrication techniques employed in this work, two-photon polymerization (2PP) and fs-laser micromachining, are schematically presented in Fig. 1(a and b), respectively.

For the 2PP, illustrated in Fig. 1(a), two scanning mirrors and a motorized stage are used to scan the laser beam through the sample. The motorized stage moves (50 nm minimal incremental motion) the sample along the beam propagation direction (z), while a pair of galvanometric mirrors deflects the beam in the x and y directions, allowing for the fabrication of three-dimensional structures. The laser beam is focused into the sample using a microscope objective. A red light emitting diode (illumination at 600–680 nm) and a (640 × 480) CCD camera are used for monitoring the fabrication in real time. We used a Ti: Sapphire laser, operating at 82 MHz that delivers ~50 fs pulses at 790 nm (40 nm bandwidth), as the excitation source for the 2PP. In the vicinity of the focal volume, the light intensity is high enough, such that the photoinitiator undergoes two-photon absorption, locally promoting the sample polymerization. After the microfabrication, the samples are immersed in ethanol to wash away all uncured resin, leaving only the fabricated microstructures adhered to the substrate.

The base resin used in the 2PP microfabrication is composed of two triacrylate monomers; tris(2-hydroxyethyl) isocyanurate triacrylate which gives hardness to the microstructure and ethoxylated(6) trimethylolpropane triacrylate which is responsible for reducing shrinkage upon polymerization. The ratio between each monomer in the resin can be chosen to tailor the final polymer mechanical properties [28]. The monomers are mixed in ethanol and then the liquid photoinitiator ethyl-2,4,6-trimethylbenzoyl phenylphosphinate is added in 3 weight% in excess [29].

The method developed for indirectly doping the microstructures with gold nanoparticles is carried out in two steps according to [30]. The first step consists of mixing the monomers with an aqueous solution of $HAuCl_4$ (2 g/l). The components were mixed in a proportion of 1 ml of the solution to 2.5 g of the resin for 1 h. After mixing, the sample is left for 24 h in a 50 °C chamber for evaporation of the solvents and then it is ready for the 2PP fabrication. The second step takes place after the microstructure fabrication and washing process. The sample is then heated to 185 °C for 35 min, which promotes the reduction of gold ions to metallic gold, with the polymer acting as the reducing agent. Also, by raising the temperature we increase the mobility of the atomic species inside the microstructure, promoting the formation of gold nanoparticles.

ZnO nanowires were prepared by a hydrothermal technique from an aqueous solution of potassium hydroxide and zinc nitrate. A glass beaker containing a homogeneous and transparent solution of the reactants was placed on a hot plate at 80 °C for about 4 h. After the reaction a milky white precipitation of ZnO nanowires was collected from the beaker and washed several times with water and ethanol. The obtained nanowires are 1–3 μm long and with diameters of approximately 100 nm. After the monomers are mixed to the phoinitiator in ethanol, we add the ZnO nanowires in a proportion of 0.5–5 wt%, mixing the components for one hour. After waiting 24 h for solvent evaporation, a viscous liquid is obtained, which is used for 2PP. The microfabrication was carried out using the apparatus displayed in Fig. 1(a), with an average power of 30 mW (measured before the objective).

For the fs-laser micromachining, presented in Fig. 1(b), we use three motorized stages to scan the sample in x, y and z directions while the beam is kept still. Two different laser systems were employed, an oscillator operating at 5 MHz with pulses of 50 fs and 100 nJ (pulse energy), and an amplified system with repetition rate of 1 kHz and pulses of 150 fs and 400 μJ (pulse energy), both systems centered at 800 nm. For the micromachining, we focused the laser beam into the sample using a microscope objective with numerical aperture (NA) of 0.65. This parameter determines the width of the focal volume and, consequently, the feature size of the micromachined area. The samples are placed on a computer-controlled x–y–z stage, which moves the sample with a constant speed, while the objective lens remains fixed, as illustrated in Fig. 1(b). The sample scan speed was 100 μm/s and 10 μm/s when using the amplified and the oscillator systems, respectively.

Glass samples containing copper or silver ions were used to obtain the respective metallic nanoparticles by fs-laser micromachining. For the copper ions we used a borosilicate glass as host matrix – ($50SiO_2$–$17B_2O_3$–$11.5MgO$–$10Na_2O$–$11.5Al_2O_3$):0.1CuO (mol%), named Cu:BSi, while for the silver a matrix composed of ($42.5B_2O_3$–$15SiO_2$–42.5BaO): $0.1CeO_2$–$0.05Ag_2O_3$ (mol%) was

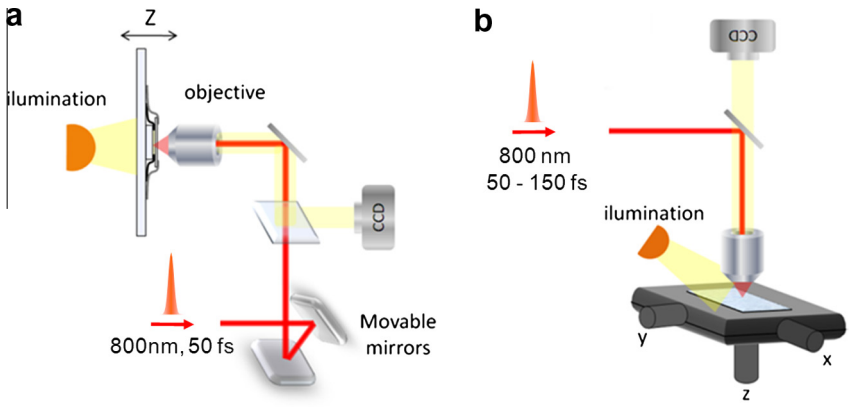

Fig. 1. Experimental setup for two-photon polymerization (2PP) (a) and fs-laser micromachining (b).

employed, named AgBBO. Both glass samples were synthesized by conventional melting–quenching technique, using high purity metal oxides and Na_2CO_3, $BaCO_3$, $AgNO_3$ as raw materials. The stoichiometric mixture of the reagents was melted in a platinum crucible, using an electric furnace open to the atmosphere. The liquid was quenched into a preheated stainless-steel mold and annealed to minimize the mechanical stress. For the copper doped glass the melting and annealing temperature/time were 1400 °C for 1 h and 400 °C for 12 h, respectively. For the silver doped glass, these temperatures were 1200 °C for 2 h and 350 °C for 24 h.

The glass transition temperature (T_g) was determined by differential scanning calorimetry (DSC), using a Netzsch STA 409C equipment, in Al_2O_3 pans, within a range of 20–900 °C with a heating rate of 10 °C/min, and in a synthetic air atmosphere. From the DSC curve of the Cu:BSi glass, we obtained $T_g = (495 \pm 2)$ °C and no exothermic peak was found, indicating that there is no formation of crystalline phases during the heating up to 900° C. The T_g of the Ag:BBO glass was determined as (597 ± 2) °C, and the onset of the crystallization peak as (694 ± 2) °C. For annealing at 650 °C, no crystalline phase was observed for times smaller than 3 h. However, for long times the β-BBO could be indexed on the X-ray diffraction pattern.

All samples obtained by two-photon polymerization and fs-laser micromachining were analyzed by optical microscopy, fluorescence microscopy, scanning electron microscopy (SEM) and UV–Vis absorption spectroscopy. The formation of metallic nanoparticles was confirmed by transmission electron microscopy (TEM).

3. Results and discussions

3.1. Hybrid nanomaterials composed of gold and zinc oxide nanostructures in a polymeric matrix

By using the indirect doping method described in Tribuzi et al. [30], we prevent the presence of gold nanoparticles during the 2PP microfabrication, which can be deleterious to the microfabrication process. SEM investigations (results not shown) evidences that the fabricated microstructures display structural integrity and smooth surface.

The microstructures doped with Au nanoparticles present a strong fluorescence, which is not observed in the non-heated $HAuCl_4$ doped microstructures, evidencing the presence of gold nanoparticles. Fig. 2 shows a confocal fluorescence microscopy image, obtained using excitation at 450 nm (40× objective), of a microstructure containing Au nanoparticles. Such results indicate that Au nanoparticles are distributed homogeneously in the microstructure bulk, since homogenous fluorescent emission has been observed from distinct *x*–*y* planes of the microstructure.

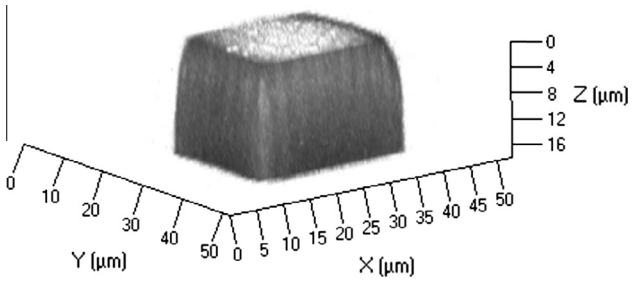

Fig. 2. Fluorescence confocal microscopy image of a microstructure containing Au nanoparticles.

Fig. 3 shows fluorescence microscopy images obtained from the emission of the microstructures under excitation with light of a wavelength of 550 nm (a), 475 nm (b) and 360 nm (c). As it can be seen in Fig. 3, we have been able to obtain emission from the microstructures covering a broadband of the visible spectrum[1], from the red (a), up to yellow (b) ending to the blue (c). The blue emission in Fig. 3(c) probably results from the fluorescence of Au nanoparticles [30], whereas the red and green emissions (Fig. 3(a and b)) are probably due to a local field enhancement of the fluorescence of the polymeric resin, since in these cases the excitation wavelength is close to the plasmon absorption band of Au, centered at 540 nm. It is important to mention that no emission is observed if there are no nanoparticles into the microstructures. These results demonstrate that microstructures fabricated by 2PP doped with metal nanoparticles could be used in applications where high emission intensity is required such as, for instance, for micro RGB displays.

Fig. 4 shows a SEM image (tilted view) of microstructures fabricated by 2PP containing ZnO nanowires. The SEM image indicates that the presence of the ZnO nanowires does not affect the 2PP process, since the microstructures present good structural integrity, indicating that the approach based on a polymer matrix containing semiconductor nanostructures is well-suited for the development of hybrid devices.

Given the interesting prospects of polymeric microstructures doped with ZnO nanowires for optoelectronic and photonic applications, we investigated the nonlinear optical properties of the fabricated microstructures by measuring the two-photon excited emission of the doped samples. In this case, the nonlinear nature of the absorption enables spatial localization of the excitation. Besides, the use of red-shifted wavelengths as excitation source

[1] For interpretation of color in Fig. 3, the reader is referred to the web version of this article.

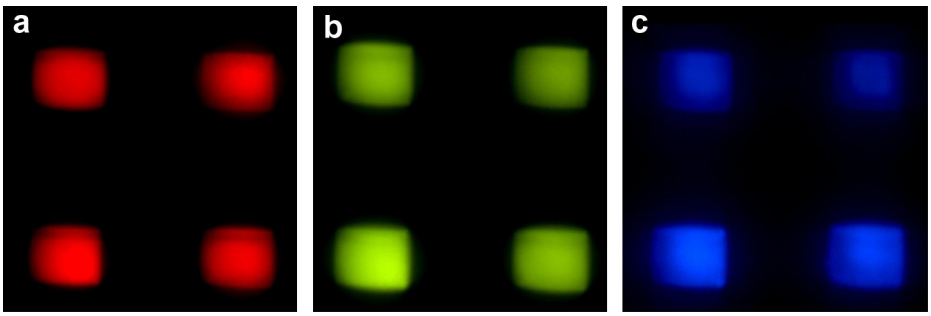

Fig. 3. Fluorescence microscopy images of two-photon polymerized microstructures containing Au nanoparticles, for excitations at 550 nm (a), 475 nm (b) and 360 nm (c).

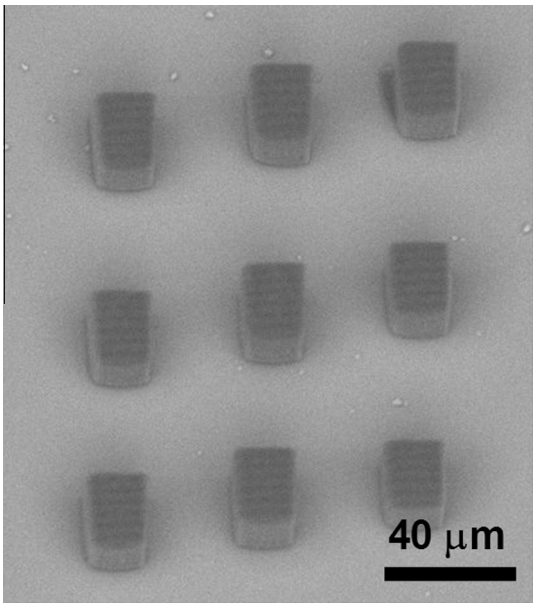

Fig. 4. SEM images of 2PP microstructures containing ZnO nanowires in a proportion of 0.5 wt%.

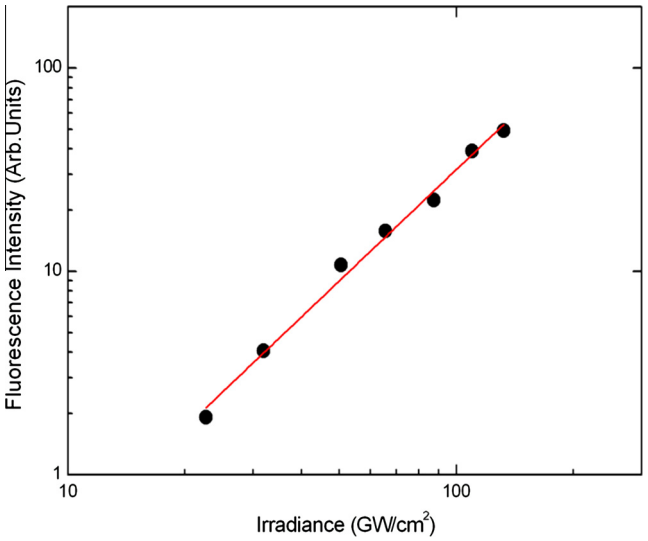

Fig. 5. Fluorescence intensity (open circles) as a function of excitation irradiance of 5 wt% ZnO doped microstructures. The linear fit in the log–log scale (solid line) yields a slope of two, revealing the two-photon absorption origin of the process.

decreases light scattering, increasing light penetration depth. To observe the fluorescence of the microstructures, we have set up a system that makes use of an optical microscope and a highly sensitive CCD camera (5-Megapixel). The two-photon excitation is carried out by applying 150 fs pulses from a Ti:sapphire amplified system operating at 775 nm and 1 kHz. After adjusting the focus of the microstructure image on the microscope, we turn on the laser excitation and collect the fluorescence images of the microstructures. This procedure is repeated for different excitation irradiances (in the order of tenths of GW/cm^2). The results were analyzed using an image processing software, from which we obtained the average emission intensity. Fig. 5 presents, on a log–log scale, the emission intensity (average value of image intensity) of the ZnO doped-microstructures as a function of excitation irradiance. The solid line in this figure represents a linear fit (in the log–log scale) having a slope of two. This quadratic dependence of the fluorescence on the excitation intensity reveals the two-photon absorption origin of the process.

3.2. Hybrid nanomaterials composed of copper and silver nanoparticles in glassy matrices

3.2.1. Copper doped borosilicate glass (Cu:BSi)

Fig. 6(a) shows the absorption spectrum of the Cu:BSi sample before irradiation with fs-pulses (as prepared). The sample has a wide absorption band in the range of 550–1000 nm, that is related to Cu^{2+} and confers the bluish color to the sample [31]. The black line in Fig. 6(b) displays the absorption spectrum of the Cu:BSi sample after irradiation with the oscillator system (5 MHz). In this case, we used a 40× microscope objective and translated the sample perpendicularly to the incident light at a speed of 10 μm/s, with an average laser power of 370 mW. Under such conditions, the sample is subjected to 1.5×10^6 pulses/spot (~3 μm) and each spot experiences a fluence of 1.6 MJ/cm^2. The irradiated area is composed of approximately 300 lines of 3 mm in length, separated by 15 μm. The absorption band observed around 570 nm in Fig. 6(b) corresponds to the plasmon band of copper nanoparticles [21,32]. It is worth mentioning that the Cu nanoparticles have been produced exclusively by the fs-laser irradiation, without the need of subsequent thermal treatment on the sample. When the Cu:BSi sample is irradiated with the amplified laser system (40× microscope objective, translation speed of 100 μm/s and average laser power of 470 mW), no evidence of the plasmon band is observed in the absorption spectrum. However, when the laser micromachined sample is subjected to a heat treatment (600 °C for 1 h), the irradiated area exhibits a plasmon band centered at 570 nm, corresponding to the presence of the Cu nanoparticles, as can be seen by the green line of Fig. 6(c). The micromachining conditions used in this case correspond to 30 pulses/spot with each spot (~3 μm) subjected to a fluence of 0.17 MJ/cm^2. As can be seen in the pictures in the insets of Fig. 6, after the production of Cu nanoparticles the irradiated area presents a reddish color. It is worthwhile to stress that the generation of Cu nanoparticles is only observed in the irradiated areas.

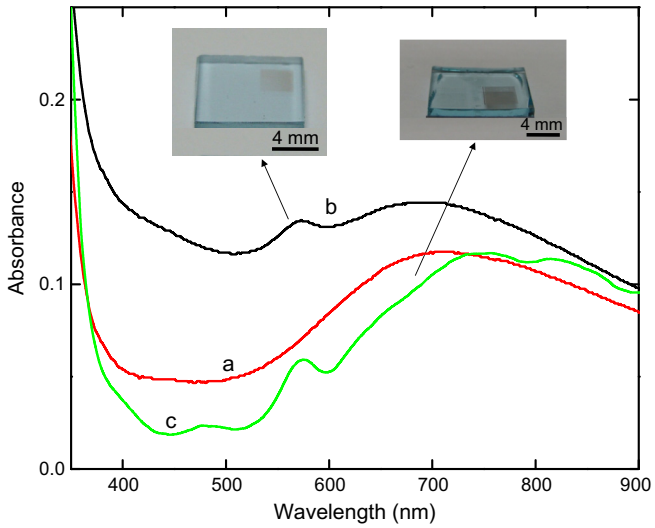

Fig. 6. Absorption spectrum of the Cu:BSi sample as prepared (a), after irradiation with the 5 MHz fs-laser (b), and after irradiation with the amplified fs-laser (1 kHz) and subsequent thermal treatment at 600 °C for 1 h (c). The insets show pictures of the irradiated sample (b and c) after the production of the nanoparticles for each case.

To further confirm the production of Cu nanoparticles in the samples, we have carried out TEM measurements, whose results are presented in Fig. 7. The inset of Fig. 7 displays the electron diffraction pattern of Cu nanoparticles, obtained for the sample micromachined with the amplified laser system and subsequent thermal treatment. The obtained diffraction pattern reveals the formation of Cu nanoparticles with cubic crystal symmetry, that corresponds to group precipitates with approximately the same crystallographic orientation.

The photoreduction of Cu^{2+} ions, and the subsequent production of nanoparticles, is a consequence of the free electrons generated by the nonlinear light-matter interaction induced by the fs-laser excitation, which results in the formation of copper atoms (Cu^0). The nanoparticles are hence obtained upon aggregation of Cu^0, which requires mobility of the neutral Cu atoms, attained by heating up the sample. Therefore, when high repetition rate laser (5 MHz) is employed, accumulative effects originated from the sequential absorption of pulses heat the irradiated region [33] promoting diffusion and aggregation of the Cu^0 atoms, leading then to the formation of nanoparticles [32–34]. On the other hand, when low repetition rates are used (1 kHz) no thermal effects are present, because the pulse energy-matter interaction time is shorter than the time necessary to transfer the absorbed energy to the lattice [1]. For this reason, in the experiments carried out with the 1 kHz laser system, we only observed the plasmon band upon laser irradiation and further external heat treatment, responsible for providing the atomic mobility for diffusion and formation of nanoparticles. Due to the very distinct pulse energies achieved with each laser system, the production of nanoparticles with the oscillator (MHz system) requires a fluence which is one order of magnitude higher than the one employed with the amplifier laser system. It is worth mentioning that reverse saturable absorption (RSA) has been observed in copper doped glasses [35]. This process may play a positive contribution on the formation of nanoparticles, once RSA implies a higher excited-state absorption cross-section which would favor the electronic transition to the conduction band. Thus, the increase of free electron generation could improve the Cu^{2+} photoreduction and the formation of the metallic nanoparticles.

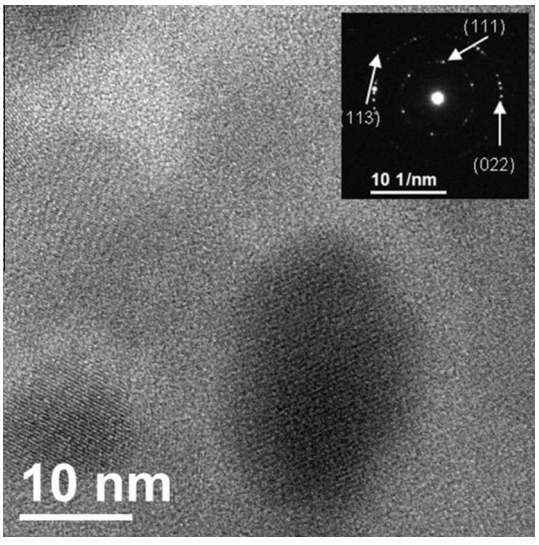

Fig. 7. TEM images obtained from the Cu:BSi sample irradiated with amplified laser system after the heat treatment. The electron diffraction pattern is shown in the inset, revealing the formation of Cu nanoparticles.

3.2.2. Silver doped barium borate glass (Ag:BBO)

In Fig. 8 we present results concerning the production of Ag nanoparticles in the Ag:BBO glass sample. The absorption spectrum of the as-prepared sample (non-irradiated) is shown Fig. 8(a), and displays its broad transparent window, including the spectral region at 800 nm, where the excitation is carried out. The black line in Fig. 8(b) exhibits results obtained for the sample irradiated using the oscillator laser system (5 MHz), whereas the blue line (c) displays the absorption spectrum obtained for the sample using the amplified system (1 kHz). For both laser systems the same 40× microscope objective was used (spot diameter of ~3 μm). The scanning speed used for the micromaching was 10 μm/s for the oscillator and 100 μm/s for the amplified laser system. For the oscillator (Fig. 8(b)) we used an average power of 270 mW, leading to a fluence of 1.1 MJ/cm^2, six times higher than the amplified system (0.18 MJ/cm^2, using 415 mW). As shown in Fig. 8, with both systems we were able to observe the resonant

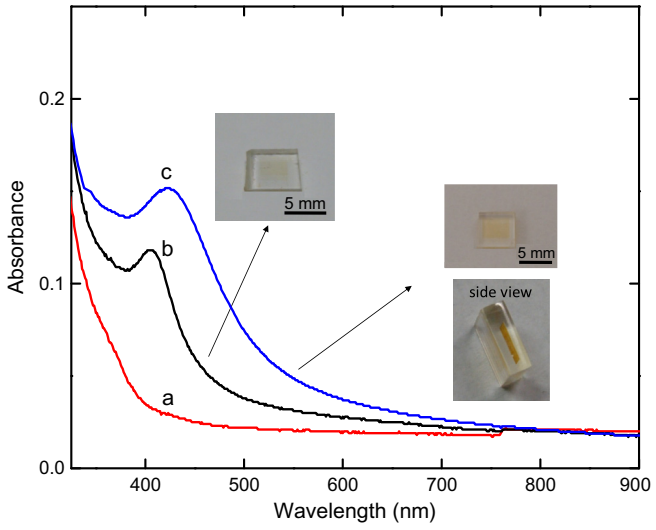

Fig. 8. Absorption spectrum of the Ag:BBO sample as prepared (a), after irradiation with the 5 MHz fs-laser (b) and after irradiation with the amplified fs-laser (1 kHz) and subsequent thermal treatment at 400 °C for 1 h (c). The insets show pictures of the irradiated sample after the nanoparticles production for each case, which displays that the nanoparticles formation occurs also in the bulk (top view).

plasmon band around 410 nm, corresponding to the presence of the silver nanoparticles. Similarly to the Cu:BSi sample, the plasmon band for the Ag:BBO sample irradiated with 1 kHz system was only observed after heat treatment (400 °C for 1 h).

The pictures in the insets of Fig. 8 shows that the production of the Ag nanoparticles occurs only in the fs-laser irradiated areas, conferring a yellowish color to it. It is interesting to note (see inset of Fig. 8) that the production of the Ag nanoparticles can be confined to the bulk of the sample, as a result of the nonlinear interaction that promotes the photoreduction of the Ag.

4. Conclusions

We employed femtosecond laser processing to produce hybrid materials, including polymeric matrices containing Au and ZnO nanostructures and borate and borosilicate glasses containing Cu and Ag nanoparticles. Specifically, we produced, by two-photon polymerization, microstructures which due to the presence of Au nanoparticles are fluorescent at red, green and blue colors through the excitation at 550, 475 and 360 nm, respectively. Red and green emissions probably arise from the local field enhancement of the polymeric resin fluorescence, while the blue emission probably corresponds to the fluorescence of the Au nanoparticles. Further studies are needed to completely understand the origin of such emissions. Another hybrid material developed by two-photon polymerization was the microstructure containing ZnO nanowire, which displayed intense fluorescence using two-photon excitation. In addition, femtosecond laser processing was also used to macromachine boro- and borosilicate glasses to induce nucleation and growth of Cu and Ag nanoparticles in the bulk of glassy matrices, which present new plasmonic absorption bands. Both high and low repetition rate lasers can be employed to produce such nanoparticles in glasses. Nonetheless, for the production of the nanoparticles using lasers with repetition rate of kHz and fluence of 0.2 MJ/cm^2 an additional heat treatment is required, while the latter in not necessary when higher fluences (6–9 times) lasers operating at MHz scale are employed. In summary, we demonstrated that femtosecond laser processing is a powerful tool to obtain hybrid nanomaterials, based on polymeric and glassy matrices containing metallic and semiconductor nanostructures, with interesting absorption and luminescent properties for designing optical and photonics devices.

Acknowledgments

We thank financial support from the Brazilian agencies FAPESP, CNPq and CAPES. T.V. acknowledges financial support by the German Research Foundation (DFG) through the research unit FOR1616 (project VO1265/7). Authors would also like to thank W. Avansi and the Brazilian National Synchrotron Light Laboratory (LNLS) for the TEM measurement.

References

[1] R.R. Gattass, E. Mazur, Nat. Photonics 2 (2008) 219–225.
[2] L. Kuna, C. Sommer, F. Reil, J.R. Krenn, P. Hartmann, P. Pachler, H. Hoschopf, F.P. Wenzl, Appl. Surf. Sci. 258 (2012) 9213–9217.
[3] D.S. Correa, M.R. Cardoso, V. Tribuzi, L. Misoguti, C.R. Mendonca, IEEE J. Sel. Top. Quantum Electron. 18 (2012) 176–186.
[4] A.Y. Vorobyev, C.L. Guo, Sci. Adv. Mater. 4 (2012) 432–438.
[5] K. Sugioka, Y. Cheng, Lab Chip 12 (2012) 3576–3589.
[6] S. Kawata, H.B. Sun, T. Tanaka, K. Takada, Nature 412 (2001) 697–698.
[7] S. Maruo, O. Nakamura, S. Kawata, Opt. Lett. 22 (1997) 132–134.
[8] F. Korte, J. Serbin, J. Koch, A. Egbert, C. Fallnich, A. Ostendorf, B.N. Chichkov, Appl. Phys. A-Mater. Sci. Process. 77 (2003) 229–235.
[9] H.B. Sun, S. Kawata, Two-Photon Photopolymerization and 3D Lithographic Microfabrication, NMR – 3D Analysis – Photopolymerization, Springer-Verlag Berlim, Berlin, 2004. pp. 169–273.
[10] C.N. LaFratta, J.T. Fourkas, T. Baldacchini, R.A. Farrer, Angew. Chem.-Int. Ed. 46 (2007) 6238–6258.
[11] K.S. Lee, R.H. Kim, D.Y. Yang, S.H. Park, Prog. Polym. Sci. 33 (2008) 631–681.
[12] S.R. Marder, J.L. Bredas, J.W. Perry, MRS Bull. 32 (2007) 561–565.
[13] S. Maruo, J.T. Fourkas, Laser Photonics Rev. 2 (2008) 100–111.
[14] M. Farsari, M. Vamvakaki, B.N. Chichkov, J. Opt. 12 (2010).
[15] A.M. Kowalevicz, V. Sharma, E.P. Ippen, J.G. Fujimoto, K. Minoshima, Opt. Lett. 30 (2005) 1060–1062.
[16] W. Watanabe, S. Sowa, T. Tamaki, K. Itoh, J. Nishii, Jpn. J. Appl. Phys. Part 2 – Lett. Express Lett. 45 (2006) L765–L767.
[17] X. Liu, D. Du, G. Mourou, IEEE J. Quantum Electron. 33 (1997) 1706–1716.
[18] D.M. Krol, J. Non-Cryst. Solids 354 (2008) 416–424.
[19] J.R. Qiu, M. Shirai, T. Nakaya, J.H. Si, X.W. Jiang, C.S. Zhu, K. Hirao, Appl. Phys. Lett. 81 (2002) 3040–3042.
[20] J.R. Qiu, X.W. Jiang, C.S. Zhu, M. Shirai, J. Si, N. Jiang, K. Hirao, Angew. Chem.-Int. Ed. 43 (2004) 2230–2234.
[21] J.M.P. Almeida, L. De Boni, W. Avansi, C. Ribeiro, E. Longo, A.C. Hernandes, C.R. Mendonca, Opt. Express 20 (2012) 15106–15113.
[22] X. Huang, S. Neretina, M.A. El-Sayed, Adv. Mater. 21 (2009) 4880–4910.
[23] Y.H. Tao, J.F. Han, C.T. Ye, T. Thomas, H.Y. Dou, J. Mater. Chem. 22 (2012) 18864–18871.
[24] J.N. Anker, W.P. Hall, O. Lyandres, N.C. Shah, J. Zhao, R.P. Van Duyne, Nat. Mater. 7 (2008) 442–453.
[25] C.J. Heo, H.C. Jeon, S.Y. Lee, S.G. Jang, S. Cho, Y. Choi, S.M. Yang, J. Mater. Chem. 22 (2012) 13903–13907.
[26] H.A. Atwater, A. Polman, Nat. Mater. 9 (2010) 205–213.
[27] A. Dev, A. Elshaer, T. Voss, IEEE J. Sel. Top. Quantum Electron. 17 (2011) 896–906.
[28] T. Baldacchini, C.N. LaFratta, R.A. Farrer, M.C. Teich, B.E.A. Saleh, M.J. Naughton, J.T. Fourkas, J. Appl. Phys. 95 (2004) 6072–6076.
[29] C.R. Mendonca, D.S. Correa, T. Baldacchini, P. Tayalia, E. Mazur, Appl. Phys. A-Mater. Sci. Process. 90 (2008) 633–636.
[30] V. Tribuzi, D.S. Correa, W. Avansi, C. Ribeiro, E. Longo, C.R. Mendonca, Opt. Express 20 (2012) 21107–21113.
[31] N.S. Rao, L.S. Rao, Y. Gandhi, V. Ravikumar, N. Veeraiah, Phys. B – Condens. Matter 405 (2010) 4092–4100.
[32] Y. Teng, B. Qian, N. Jiang, Y. Liu, F.F. Luo, S. Ye, J.J. Zhou, B. Zhu, H.P. Zeng, J.R. Qiu, Chem. Phys. Lett. 485 (2010) 91–94.
[33] Y. Dai, G. Yu, M. He, H. Ma, X. Yan, G. Ma, Appl. Phys. B-Lasers Opt. 103 (2011) 663–667.
[34] Y. Teng, J.J. Zhou, F.F. Luo, G. Lin, J.R. Qiu, J. Non-Cryst. Solids 357 (2011) 2380–2383.
[35] D. Manzani, J.M.P. Almeida, M. Napoli, L.D. Boni, M. Nalin, C.R.M. Afonso, S.J.L. Ribeiro, C.R. Mendonça, Plasmonics (2013), http://dx.doi.org/10.1007/s11468-013-9585-z.